Christine Bonthius
GISWR – Maidment

Morphodynamics of the Madeira River in Brazil

Introduction

Channel patterns of fluvial systems exist in a continuum acted upon by geomorphic and hydrologic conditions (Nanson and Knighton 1996). Alterations of these conditions result in a different manifestation of channel pattern and the transition from one to another. The thresholds that instigate such changes are not clear, though it has been recognized that distinct conditions are characteristic of certain channel patterns. Four distinct channel patterns have been identified: straight, meandering, braided, and anastomosing, the last of which is poorly understood (Knighton 1998). The category of anastomosing rivers also encompasses the more complex classification of anabranching rivers, or those that develop a structure of multiple channels. These systems are representative of the largest fluvial systems on the planet, or "mega-rivers", which demonstrate an exclusively anabranching channel pattern (Latrubesse 2008). The Madeira River, the fifth largest river in the world, is classified as anabranching, though sections of the river demonstrate combinations of less complex channel patterns. An investigation of the hydraulic conditions in these areas of differentiated patterns may indicate the presence of a threshold in the Madeira River and may shed light on the stability of anabranching rivers.

The analysis for this project required spatial component to adequately describe hydraulic processes over a span of distance. Thus, modeling data of geomorphic and hydrologic variables in a Geographic Information System (GIS) was an effective and helpful tool for both a qualitative and quantitative characterization of the Madeira River.

Study Area

The Madeira River Basin in located in the western region of the Amazon River Basin in the states of Rondonia and Amazonas in Brazil. The Madeira River is the largest tributary of the Amazon River, and has an average annual discharge of approximately 32,000 cubic meters per second. It is formed by the headwaters of the Bení and Mamoré Rivers whose headwaters are in the Bolivian Andes. The river begins in the Andes and flows north-northeast for approximately 700 kilometers before it enters the Amazon River just upstream of Manaus. It is considered to be a "white water" river, as it is sediment-rich and has a high suspended sediment load. The Madeira River has an average annual sediment load of approximately 33 million tons per square kilometer per year, a value that is about half of the Amazon River's annual sediment output (Latrubesse et al 2005). The channel pattern is primarily anabranching with sinuous second order channels. Other channel patterns, including meandering and straight single channels, are also present, indicating that the river may be on a hydraulic or geomorphologic threshold in channel pattern formation.

The selected study reach is located downstream of the city Porto Velho in Rondônia and spans a distance of about 140 river kilometers (Figure 1). The reach contains one tributary, the Jamarí River, which contributes minimal discharge to the area. The study reach contains four distinct channel patterns in the reach: a meandering stretch, a box-shaped meandering stretch, a straight single channel stretch, and an anabranching stretch.

Figure 1: The study area is indicated in the yellow box (below). The reach spans approximately 140 river kilometers downstream of the city of Porto Velho (Rondônia, Brazil).

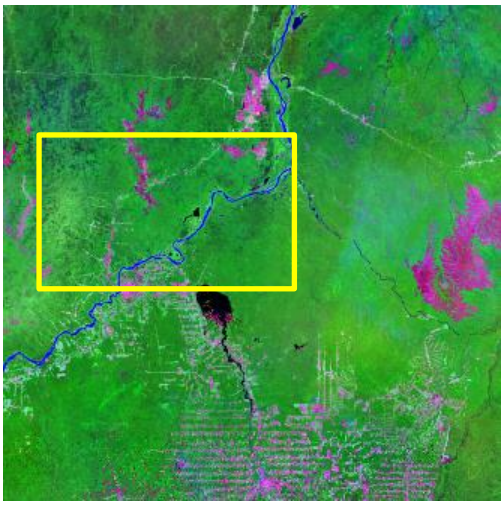

The variety in channel pattern seems to be constrained to this one area in the basin, allowing for interesting comparisons in geomorphologic and hydraulic conditions in the study reach.

Currently, two hydroelectric projects are under construction on the Madeira River just upstream of Porto Velho. The Jirau and Santo Antonio hydroelectric complexes are expected to be fully operational by January 2013. These projects are expected to be a significant contributor of energy to the northern region of the country (Table 1). The filling of the reservoirs behind each dam is to begin immediately after dam operations. The Jirau complex will require a reservoir with a volume of 258 square kilometers and an area of $2.015x10^6$ cubic kilometers. The Santo Antonio complex will create a reservoir with an area of 271.3 square kilometers and a volume of $2.075x10^6$ cubic kilometers. Both complexes have an expected life span of approximately 70 years, a surprisingly short amount of time (Relatório do Impacto Ambiental 2007).

Table 1: Technical Specs of the Hydro-electric Complexes on the Madeira River

Technical Fact	Jirau Complex	Santo Antonio Complex
Area of Reservoir (km^2)	258	271.3
Volume of reservoir (km^3)	2.015×10^6	2.075×10^6
Energy Potential (MW)	3.3	3.150
Turbine Type	Bulb	Bulb
Extent of Transmission Line (km)	120	5

Geomorphology

In the study reach, a variety of morpho-stratigraphic units influence the channel morphology (Figure 2). Topographic relief of Tertiary age in the upstream reaches of the area shows a pattern of interspersed small undulating hills and depressions that vary between ten to twenty meters deep. On the northern side of the river in this area, the plain gains elevation and

forms elevated plateaus. Residual unstructured mountains are visible alongside small escarpments, remnant ridges aligned in crests, and dissected ancient plateaus. A ridge, now degraded into gently sloping hills, bisects the river and creates a series of rapids upstream of Porto Velho. The right side of the river is characterized by a plain-like surface and the absence of residual relief. This surface appears to have been eroded by a drainage network of that formed long, wide valleys and flat summits.

The Madeira River maintains an active floodplain with aggradational features and geomorphic units of Quaternary age; units of Tertiary ages are located further from the floodplain. In-channel features include sand bars and alluvial islands. Alluvial islands are isolated areas of the floodplain and are vegetated stable features in the landscape for the time period of the analysis. The average length of islands is 3.286 kilometers and the average width is 1.088 kilometers, yielding an average length-width ratio of 3.224. Temporal stability is characteristic of these features. Seven islands were identified in the study reach in 1986, and eight were detected in 2010, as one had been excised from the floodplain by the activation of a secondary channel.

Figure 2: Geomorphic units in the study area of the Madeira River. Units are coded by age, with A3 units as the youngest geomorphic units, and A2 units as older units. In the study area (shown in the yellow box), much of the channel is laterally constrained by these units.

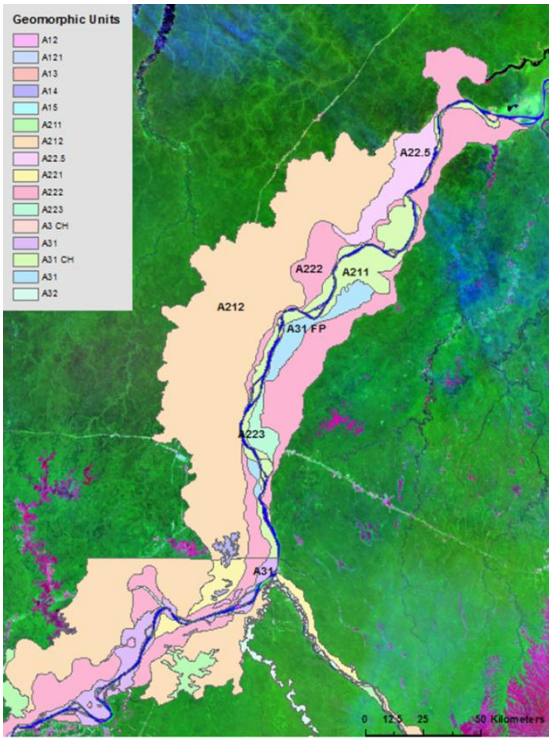

Hydrology

Discharge and gauge height data was collected the Brazilian National Water Agency for four gauges (Abuña (1976-2004), Porto Velho (1967-2011), Manicoré (1967-2011), and Fazenda Vista Alegre (1967-2011)) in the Madeira River Basin. Hydrographs for the Madeira River at four gauge stations indicate that the discharge of the Madeira River is highly seasonal. The maximum discharge (average = 58,217.065 m^3/s) occurs during the wet season between April

and May, while the minimum discharge (average = 6347.871 m^3/sec) occurs during the dry season between September to November (Figure 3). The Madeira River drains more than one climatic zone, creating a complex hydrologic pattern reflective of various ecosystems from the Andean Mountains to the tropical lowlands of the Amazon Basin.

Figure 3: Hydrograph of average monthly discharge at Porto Velho

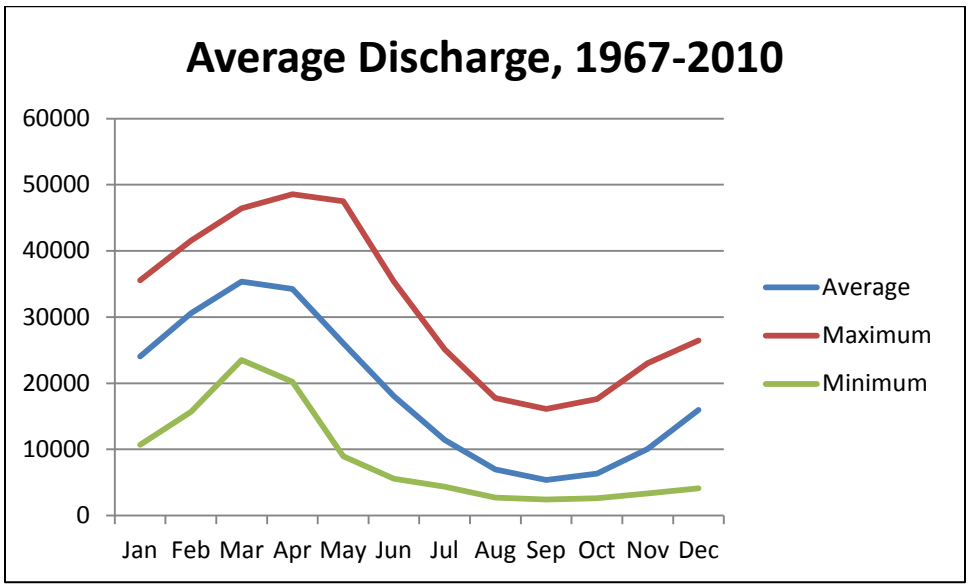

Sedimentology

Sediment carried by Madeira River is 25% clay, 60.6% silt, 12% fine sand, 2.5% medium sand/gravelly sand (Relatório dos Impactos Ambiental 2007). Overall, sediment is considered to be a fine texture. Measurements of suspended sediment concentration show that the average value is 720 mg/l, with a maximum of 3500 mg/l and a minimum of 12 mg/l. Generally, sediments on the right side of the river have a larger average grain size (d50 = 19.268 µm) than those on the left side of the river (18.577 µm). Bed sediment grain size seems to reverse pattern, with the larger average grain size found on the left bank (348.804 µm) as opposed to the right bank (301.536 µm).

Once the Madeira River is impounded, the rate of loss of sediment in the water will be 19% (year 1), about 5% (year 15) and then below 1% (year 30). This process will lead to the intensification of erosion upstream of the reservoir, potentially compromising the banks of the river in the first few kilometers of the river behind the dam (Relatório dos Impactos Ambiental 2007).

Data and Methodology

The analysis of this project relied on data collected from satellite imagery (LandSat5 Thematic Mapper bands 1, 2, 3 and 5) and on field data collected from the Madeira River using an Acoustic Doppler Current Profiler (ADCP). Much of the data had to be created for the multi-temporal and spatial analysis of morphological characteristics of the channel.

Coordinates for the beginning and ending points of each transect were collected in the field with a DGPS in the WGS1984 datum. These coordinates were used to initially create a Keyhole Markup Language (.kml) code, which was then converted into a feature class in ArcGIS with the **KML to Layer** tool. This created a new layer file, which I converted into a feature class by **Exporting the Data** and specifying the format in which to save it. I chose to save it as a shapefile for the ease of manipulating vector data. The data used for Acoustic Doppler Current Profiler (ADCP) analysis was collected during a field campaign in July 2011. The data was initially in .000 format. These files were processed first using the Teledyne TRDI WinRiverII software to create an accompanying ASCII file for the data in each transect. Hydraulic variables (water velocity, suspended sediment concentration, and water discharge) were mined from these outputs and entered into an Excel table. This table was then **joined** to the shapefile of the ADCP transects that had previously been created. The ASCII files were then processed using the Velocity Mapping Toolbox (VMT), which was created by the USGS (Parsons et al 2012). Outputs of the VMT include figures of a planform view of depth-averaged velocity vectors, figures of cross-sectional views of velocity magnitudes and secondary currents.

The software also offers the option to output tabulated bathymetry values for each ensemble of values. These depths where exported into an Excel table, which was imported into ArcGIS. I used the **Display XY Coordinates** function to display the data for each transect, then exported them as shapefiles. The shapefiles of the transects were then combined using the **Merge** function to create a single shapefile of all the bathymetric profiles. The shapfile was then **projected** it into the coordinate system of previously created files (UTM 20S). Points were displayed as quantitative values in five classes using the Jenks Natural Breaks classification method. A bathymetric color ramp was used to differentiate depths within each transect.

Geomorphic maps were created with reference to composites of LandSat 5 TM (Thematic Mapper) imagery, which were stacked with Bands 1, 2, and 3 as the red, green, and blue levels, respectively. My analysis required the use of eight different LandSat 5 TM images, which were downloaded in GeoTIFF formats. The images first required the reclassification of pixel values to assign values of "no data" to similar values. To do this, I used the **Reclassify** tool to set all pixels with a brightness value of 256 to NoData. The images were then mosaicked together using the **Mosaic to New Raster** tool in ArcGIS. Geomorphic units were delineated from **Georeferenced** images of geologic and geomorphic maps created by the Brazilian government.

I collected data from the month of July for the years 1986, 1998, and 2010 for a multi-temporal analysis of channel morphology in the selected study reach. The above process was repeated for each set of LandSat5 TM images. Then, the channel margins and the in-channel features of interest (vegetated islands) were digitized. This was done by creating and editing new shapefiles. Fields were added in the attribute table for attributes of island length, width, area, length-width ratios, and type of origin. The first four fields were filled in using the **Field Calculator** in ArcGIS as ratio type attributes with a "float" data type (precision 5, scale 2). The final field was filled with a string, or text, type attribute of either A (for aggradational features) or D (for degradational features).

Data from the Shuttle Radar Topography Mission (SRTM) was downloaded from the United States Geological Survey (USGS) viewer "Global Data Explorer". The selected area of interest in the Amazon Basin was downloaded in .TIF format. I elected to use SRTM data at a spatial resolution of 90 meters, and required 54 tiles to completely capture the area of interest. The file came defined and projected in the Universal Transverse Mercator (UTM) projection, zone 20N, with the datum WGS 1984. This file was then projected to match a previously created

file using the same projection, but that used the zone 20S. Once projected with the **Project Raster** tool, the file became usable for elevation and terrain analysis. Applying the **Hillshade** function amplified the contrast in the topography, which is lowland terrain. This allowed for a sharpened perspective off relatively small changes in an area of very low elevation and a refined distinction in geomorphic units.

Working in a remote area has its challenges in that, aside from satellite imagery, the majority of spatial information and data needs to essentially be created. Another limitation lies in the fact that the quality of your analysis is inherently reliant on the quality of the data used. During the field campaign in July 2011, problems with equipment recordings were observed, especially in the collection of Digital Global Positioning System (DGPS) coordinates for the ADCP transects. Correctional factors had to be applied for various data observations, which have been accounted for in the data. Future work has plans to anticipate and mitigate many of the issues previously encountered in the field.

Results

The analysis of multi-temporal imagery confirmed the hypothesis that the Madeira River demonstrates overall geomorphic stability for the selected time period of study. Channel stability was assessed by measuring channel widths every two river kilometers for the selected study reach, quantifying the number and dimensions of islands in the channel, and examining the processes of island excision or accretion and channel abandonment in the reach. This process was repeated for the imagery datasets from the years 1986, 1998, and 2010. As the channel is laterally constrained, river channel widths remained relatively unchanged. In 1986, the average channel width for the entire study reach was 1.15 kilometers, and in 2010 the average width was 1.21 kilometers. A slight increase was seen due to the excision of a small island during the thirty year time span, but the overall difference is not significant. There were seven islands in the channel in 1986, and eight islands in 2010 with overall average length-width ratios of 3.22 and 3.07 respectively. One island had been added to the channel via excision of the floodplain. Length-width ratios showed a slight decrease over time, indicating that erosional processes may be dominating the system.

Figure 4: Digitized islands in the channel of the study reach in 1986. Lengths and widths of each feature were recorded in the attribute table of this feature. Length-width ratios were calculated using the field calculator in ArcGIS.

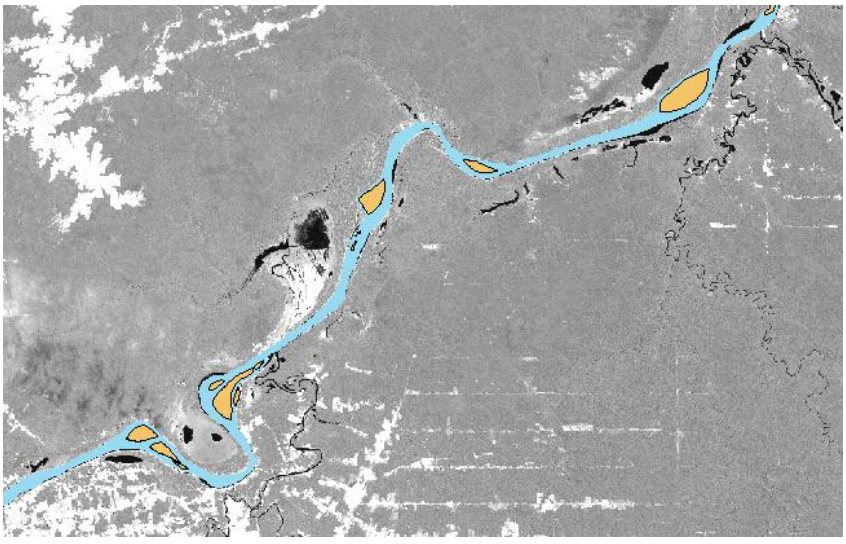

Bathymetry of the transects was displayed in ArcGIS as points with a depth value. This allowed for the visualization of channel depth variation through the study reach. Patterns of increased depths were seen in the meandering reach of the study area. When comparing these observed trends in channel depths to the figures created by the VMT, a series of transects with an exaggerated deepening on the cut-bank becomes apparent. The figures that of depth-averaged velocity vectors and of secondary current patterns indicate how flow is physically affected by, and affects, these conditions. Flow vectors in this section are deflected toward the bed, indicated by the splay of vectors that point seemingly backward. Secondary currents show a complex convergent pattern with a preferential flow direction toward the bottom of the channel. Consequently, it seems that flow direction, and perhaps depositional patterns, may play a key role in the deepening of this section. The section of minimum average depths (6.66 meters) is found in the middle section of the study reach, which is constrained by geomorphic units. An analysis of the bathymetry of the area reveals what appears to be a pool-riffle series, where the area of deepening in the channel alternates through the study area. This is also reflected in the convergent and divergent gyres seen in the patterns of the secondary currents.

Figure 5: Bathymetry of the channel in the meandering reach. Maximum depths are in red with minimum depths in green.

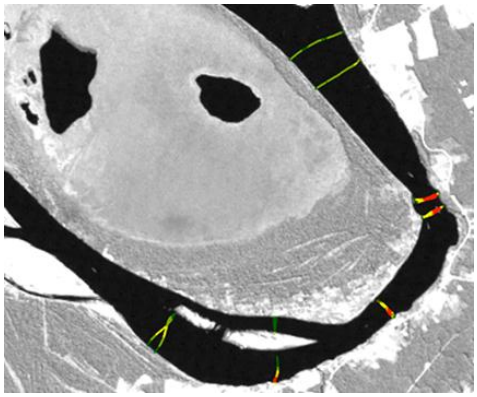

Channel widths in current conditions proved to be a worthwhile variable for analysis, especially when in incremental series corresponding to channel pattern. Channel pattern morphology was divided into three separate and distinct types within the study reach that reflects the environmental conditions in which that process operates: meandering, confined meandering in a box-shaped curve, and anabranching. The meandering reach shows pronounced curvature and elongation into the floodplain. The confined meandering seems to reflect a similar process as the meandering stretch in which the river seems to be attempting to cut into the floodplain. However, the channel is laterally constrained by geomorphic units on the floodplain, specifically remnant terraces and Pleistocene aged units, which constrain its extent of curvature. As a result, the channel manifests as a box-shaped curve with straight reaches as it directionally shifts. The third reach is a purely anabranching stretch in which the primary single channel is bifurcated into two channels by a large vegetated island. These two channels operate as two independent systems.

The distributions of channel widths in these stretches reflect these morpho-stratigraphic units and constraints. In the meandering reach, channel widths at the beginning of the stretch are approximately 1.17 kilometers. As the channel passes through a constraining unit, widths

consistently decrease. The minimum channel width is reached about 22 kilometers downstream where it narrows to a width of 0.61 kilometers. This minimum width corresponds to the greatest depth observed in any of the three identified reaches. Depth at this point reaches 24.31 meters, indicating a downward carving process may be a response to lateral constriction. After reaching the minimum width, the channel then begins to widen as the river extends its meander into the more erodible floodplain. Channel widths increase dramatically at river kilometer 34, where it reaches a maximum value for the entire study reach at 5.91 kilometers. This meandering stretch has the greatest variability in channel width values, and has an average value of 1.95 kilometers. The constrained meandering section shows markedly less variation in channel widths. The minimum channel width of the section is 0.89 kilometers and the maximum is 2.41 kilometers; average channel width for the section is 1.36 kilometers. The values for the channel width do not reach the maximum values as seen in the true meandering section because of the presence of less erodible floodplain units. Consequently, very few islands exist in this section, which reduces the width of channel measurements. The anabranching reach shows a similar variation in channel widths as the meandering stretch. The minimum channel width is seen at the beginning of the stretch with a measurement of 0.82 kilometers. The maximum width is 4.69 kilometers. The stretch has an average channel width of 1.90 kilometers, which was recorded at a point with an alluvial island.

Channel widths along the river channel are not important as only a morphological parameter for also as a correlated variable paired with water velocity. Water velocity measurements for each ADCP transect were plotted in ArcGIS as the quantitative descriptive variable. The transects were represented by a single value of the average velocity of the entire transect. This allowed for the spatial analysis of velocity distribution through the study area and the three areas of distinct channel patterns. When comparing the values of velocity with channel width, hydraulic and morphologic relationships appeared. In the meandering reach, for example, flow velocity decreased as channel width decreased. At the minimum channel width, flow velocity was also minimized at 0.28 meters per second. As the channel widened, velocity increased as well. The maximum flow velocity of 1.23 meters per second was observed at the maximum channel width in this reach. A similar pattern of loss and gain of velocity was seen in the confined meandering reach, though the variation was not as pronounced. Initial velocity in the box-shaped meander is 1.13 meters per second, and velocity decreases to 0.78 meters per second at the minimum channel width. After this point, water velocity increases again to 1.09 meters per second. The water velocity does not recuperate all the velocity that it has lost in this section. In the anabranching reach, no distinct pattern of flow velocity is evident. Water velocity ranges between 0.76 and 1.0 meters per second throughout the reach with no significant loss or gain throughout the stretch. Water velocity, however, is greater at the end of the reach than at the beginning. Initial flow velocity is 0.81 meters per second and terminal velocity is 0.97 meters per second. Water velocity slowly but consistently increases through the anabranching reach; no decrease within the reach is observed (Figure 6).

Figure 6: Spatial distributions of velocity (m/s) and channel widths (in meters versus river kilometers).

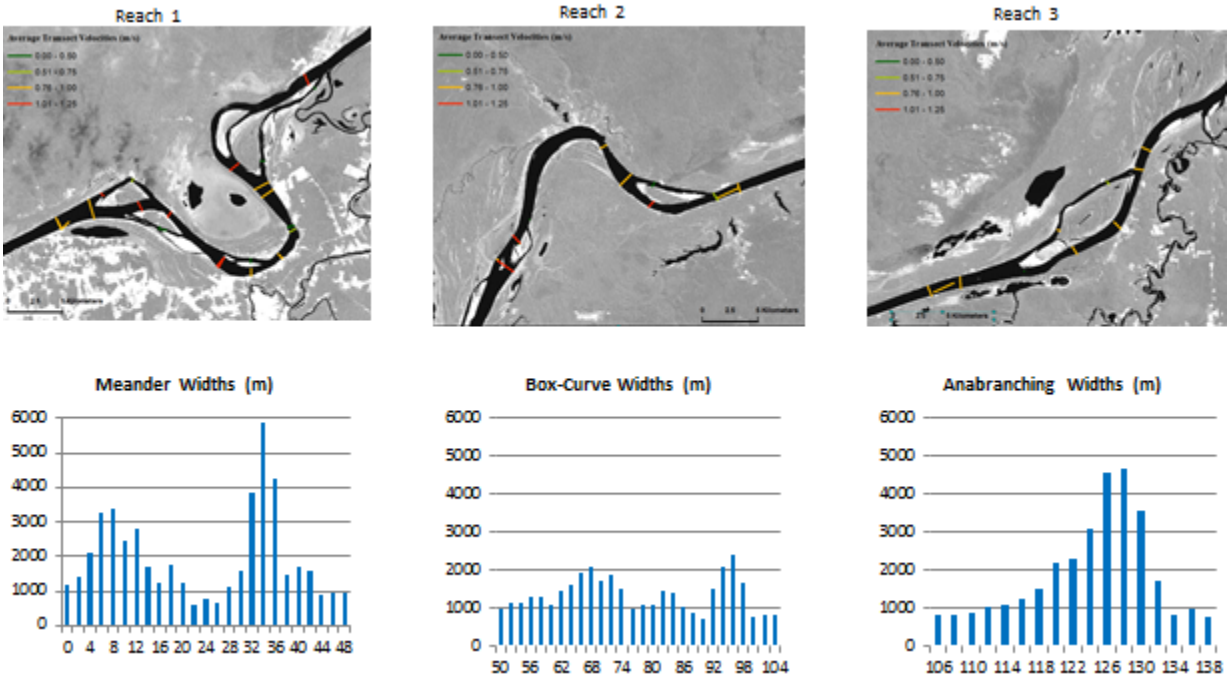

A spatial perspective on the distributions of channel morphology and hydraulic sheds light on the interactions between the geomorphology and hydrology in the study area. While the relationships between channel width and bathymetry and channel pattern is interesting, it is the link between channel width and flow velocity that best characterizes the seemingly connected exchanges in energy losses and gains. As a channel narrows in a meander, velocity is lost. In turn, as a channel widens, flow velocity is increases. Often, it seems that the widening and narrowing of the channel is a response to the fluxes in energy in the water flow. The channel widths, when looked at in a single series for the entire study reach, show a wave-like tendency. This sinusoidal trend prompts further questions regarding channel frequency and the wavelengths of channel patterns in this fluvial system, and may also determine the magnitude of the morphologic and hydraulic threshold that dominates channel pattern in the Madeira River.

Conclusions

The use of Geographic Information Systems has allowed for the identification of preliminary geomorphic and hydraulic relationships in areas of distinct channel pattern on the Madeira River. Within the study reach, three stretches were identified based on channel pattern, and the geomorphic and hydraulic relationships analyzed in each. Clearly, channel pattern and flow velocity vary in space and over the distance of the channel. These variations are seen in the differences in channel widths and the flow velocities. Bathymetry also offers insight into the controls on water flow and the secondary flows that influence flow directionality within the channel. These conditions are critical for understanding the manifestation of channel pattern as a function of its hydraulic conditions. At this point off research, only a case study of three

stretches on the channel has been analyzed. Collecting more transect data will expand the area and increase the resolution of hydraulic information available.

Future work in this area will seek to find a way to represent the distributions of hydraulic variables, such as flow velocity and direction and suspended sediment concentration, in a three-dimensional way. As of now, the only way to represent the value of this variable in each transect is by a single value. These values, however, vary both horizontally and vertically within the same transect. Analysis would greatly benefit from the visualization of the output of hydroacoustic technology in a three-dimensional yet spatially distributed layout.

References

Knighton, A.D. 1998. *Fluvial Forms & Processes: A new perspective*. Hodder Education: Great Britain.

Latrubesse, E.M. 2008. Patterns of anabranching channels: The ultimate end-member adjustment of mega rivers. *Geomorphology*, **101**, pp. 130-145.

Latrubesse, E.M, Stevaux, J.C., and Sinha, R. 2005. Tropical Rivers. *Geomorphology*, **70**, pp. 187-206.

Nanson, G.C. and Knighton, A.D. 1996. Anabranching rivers: Their cause, character and classification. *Earth Surface Processes and Landforms*, **21**, pp. 217-239.

Parsons, D. R., Jackson, P. R., Czuba, J. A., Oberg, K., Mueller, D. S., Rhoads, B. L., Best, J. L., Engel, F. L., Johnson, K. K., Riley, J. D. (in review). Velocity Mapping Toolbox (VMT): A processing and visualization suite for moving-vessel ADCP measurements. Earth Surface Processes & Landforms.

Relatório dos Impactos Ambiental dos Aproveitamentos Hidroeléctricos de Santo Antônio e Jirau, no Rio Madeira, Estado de Rondônia. 2007.

Spatial Data

LandSat5 Thematic Mapper. Earth Explorer. Accessed October 15, 2012. www.earthexplorer.usgs.gov.

SRTM (90 meter resolution) Global Data Explorer Accessed Nov. 6, 2012 http://gdex.cr.usgs.gov/gdex/